

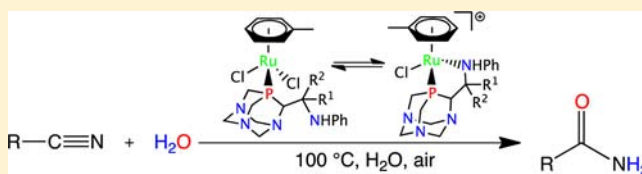
Hemilabile β -Aminophosphine Ligands Derived from 1,3,5-Triaza-7-phosphaadamantane: Application in Aqueous Ruthenium Catalyzed Nitrile Hydration

Wei-Chih Lee, Jeremiah M. Sears, Raphael A. Enow, Kelly Eads, Donald A. Krogstad,[†] and Brian J. Frost*

Department of Chemistry, University of Nevada, Reno, Nevada 89557-0216, United States

S Supporting Information

ABSTRACT: A series of β -aminophosphines derived from 1,3,5-triaza-7-phosphaadamantane (PTA) are described. PTA-CHPhNHPH (1), PTA-CH(*p*-C₆H₄OCH₃)NHPH (2), and PTA-CPh₂NHPH (3) were prepared in good yield (62–77%) by reaction of lithiated PTA with the corresponding imine followed by hydrolysis. Compounds 1 and 2 were synthesized as pairs of diastereomers which were separated by successive recrystallization from THF/hexane. Compounds 1–3 are somewhat soluble in water (S_{25}° = 4.8 (1), 4.9 (2), 2.7 (3) g/L). Upon coordination to Ru(II) arene centers both monodentate (κ^1 -P) [RuCl₂(η^6 -toluene)(1–3)] and bidentate (κ^2 -P,N) [RuCl(η^6 -toluene)(1–3)]Cl coordination modes were observed. Ru(II) arene complexes 4–6 exhibited hemilabile behavior transitioning between κ^1 -P and κ^2 -P,N coordination upon change in solvent or addition of a coordinating ligand such as Cl[−] or CH₃CN. Complexes (4–6) were found to be active air stable catalysts for the aqueous phase hydration of various nitriles with TOF up to 285 h^{−1} and TON of up to 97 000 observed.



INTRODUCTION

There has been a growing interest in the development of aminophosphine ligands, many of which have shown good catalytic performance for a broad range of organic transformations,^{1–11} e.g., (transfer) hydrogenation,^{12–18} hydroformylation,^{19–21} and hydrosilylation.^{22–25} Aminophosphines are potentially hemilabile ligands, especially if the amine group is sufficiently bulky.³ Hemilabile κ^2 -P,N complexes of aminophosphines are of interest in catalysis since the labile amine group can be displaced by substrate, allowing catalysis to proceed, and can potentially increase catalyst lifetime.

Nitrile hydration is an atom economical method to convert nitriles to amides. The mechanism is generally assumed to involve coordination of the nitrile to the metal center, necessitating an open coordination site.²⁶ Water may or may not coordinate to the metal prior to nucleophilic attack on the nitrile carbon. Amide dissociation has been implicated in catalyst deactivation or inhibition.²⁶ Both the requirement of an open coordination site and the need to remove coordinated product make hemilabile ligands intriguing for nitrile hydration.

A variety of transition metal complexes have been utilized as effective catalysts,^{26–29} for example, [Cp₂Mo(OH)(H₂O)]⁺,^{30,31} *cis*-Ru(acac)₂(PPh₂Py)₂,³² and [PtH(PMe₂OH){(PMe₂O)₂H}].³³ Ruthenium has become one of the most highly explored metals for nitrile hydration with ruthenium arene compounds as some of the most efficient and versatile catalysts with high substrate tolerance for the hydration of nitriles.^{26,34–40}

The air-stable and water-soluble aminophosphine 1,3,5-triaza-7-phosphaadamantane (PTA) has received attention in recent years mainly due to medicinal interest.⁴¹ Transition

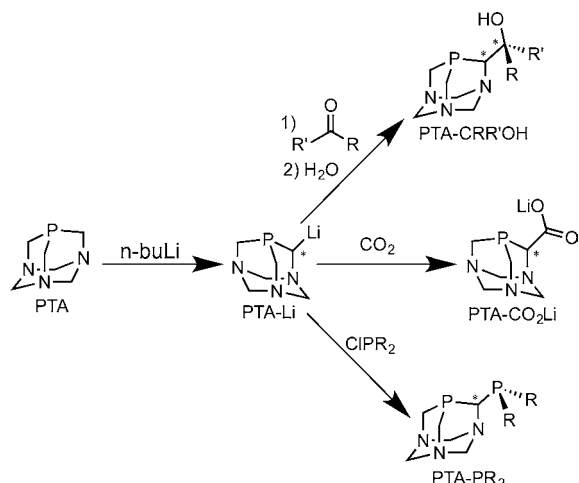
metal complexes of PTA have been used for a range of catalytic transformations,⁴² e.g., hydrogenation of arenes⁴³ and CO₂/bicarbonate,⁴⁴ transfer hydrogenation of α,β -unsaturated carbonyls,^{45,46} atom transfer radical addition,^{47,48} hydroformylation of 1-decene,⁴⁹ and hydration.^{35,39,50,51} We recently published details that [Ru(PTA)₄Cl₂] is a highly active and recyclable catalyst for nitrile hydration.⁵⁰ Cadierno and co-workers previously reported that a series of ruthenium complexes of PTA and derivatives, including [RuCl₂(η^6 -arene)(PTA)], were efficient catalysts for aqueous nitrile hydration.⁵¹ The excellent efficiency was attributed to the ability of PTA to serve as a hydrogen bond acceptor to activate water.

Our group has been interested in upper-^{52,53} and lower-rim⁵⁴ modifications of PTA maintaining the heterocyclic cage. Functionalization of the upper rim has been demonstrated by us and others through lithiation of PTA followed by reaction of PTA-Li with various electrophiles including chlorodiphenylphosphine,⁵² CO₂,⁵³ and aryl ketones and aldehydes, Scheme 1.^{53,55–57} Herein we continue this work with the synthesis of a series of β -aminophosphines obtained through the addition of imines (R¹R²C=NPh) to 1,3,5-triaza-7-phosphaadamantan-6-ylolithium (PTA-Li). These functionalized PTA derivatives were coordinated to ruthenium arene centers, and their activity for nitrile hydration is reported.

Received: May 31, 2012

Published: January 28, 2013

Scheme 1

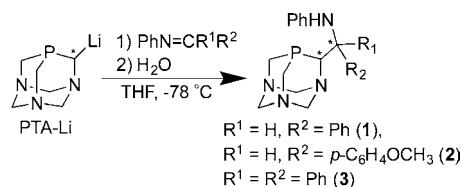


RESULTS AND DISCUSSION

The β -phosphine alcohol derivatives of PTA previously reported (Scheme 1, PTA-CRR'OH) coordinate to metals in a monodentate fashion with some evidence of bidentate coordination.^{53,55–57} We were interested in developing ligands which would be able to coordinate metals in a bidentate fashion ideally with hemilabile behavior. The β -aminophosphines described below were designed to be able to weakly chelate a metal center serving in a hemilabile manner.

Ligand Synthesis. Synthesis of ligands 1–3 was performed by adding a THF solution of the corresponding imine to a cold suspension of PTA-Li in THF followed by quenching with water (Scheme 2). The ligands were isolated as pale yellow

Scheme 2



powders in 62–77% yield and characterized by IR spectroscopy, ESI+ mass spectrometry, ^1H , $^{13}\text{C}\{^1\text{H}\}$, and $^{31}\text{P}\{^1\text{H}\}$ NMR spectroscopy, and single-crystal X-ray analysis. ^1H and ^{13}C resonances were assigned by analyzing ^1H , $^{13}\text{C}\{^1\text{H}\}$, ^{13}C DEPT (90° and 135°), COSY, HMQC, and HMBC spectral data of 1–3. The resulting β -aminophosphines are readily soluble in common organic solvents, e.g., methanol, acetone, tetrahydrofuran, chloroform, dichloromethane, toluene, and acetonitrile. Compounds 1–3 are slightly less soluble in water ($S_{25^\circ} = 2.7$ – 4.9 g/L, Table 1) than the β -phosphino alcohols previously reported by us ($S_{25^\circ} = 5.9$ – 11.1 g/L).⁵³ Similar to other upper-rim substituted PTA derivatives, compounds 1–3 are air-stable in the solid state; however, they oxidize slowly in solution. The oxidation of 1–3 in CDCl_3 was monitored by $^{31}\text{P}\{^1\text{H}\}$ NMR spectroscopy; after 6 weeks in solution ~6%, 9%, and 4% of the phosphine oxides of 1, 2, and 3, respectively, were observed.

Treatment of PTA-Li with $\text{PhN}=\text{CPh}_2$ provided a racemic mixture of 3 with a single $^{31}\text{P}\{^1\text{H}\}$ NMR resonance at -97.7 ppm in CDCl_3 . No diastereomeric selectivity was observed for the addition of $\text{PhN}=\text{CHC}_6\text{H}_5$ or $\text{PhN}=\text{CHC}_6\text{H}_4\text{OCH}_3$ to

Table 1. $^{31}\text{P}\{^1\text{H}\}$ NMR Spectroscopy and Water Solubility Data for a Series of PTA Derivatives

ligand	$^{31}\text{P}\{^1\text{H}\}^{a,b}$	M mol/L	$S_{25^\circ\text{C}}$ g/L
PTA ⁶⁷	-102.3 (-12.5)	1.5	235
PTA-CHPhNHPh (1)	-102.4 , -105.9 (-2.9 , -5.7)	0.0142	4.8
PTA-CH(<i>p</i> - $\text{C}_6\text{H}_4\text{OMe}$) NHPh (2)	-102.1 , -105.9 (-2.9 , -5.7)	0.0133	4.9
PTA-CPh ₂ NHPh (3)	-97.7 (-1.5)	0.0065	2.7
PTA-CPh ₂ OH ⁵³	-95.5 (-3.46)	0.0174	5.9
PTA-C(<i>p</i> - $\text{C}_6\text{H}_4\text{OMe}$) ₂ OH ⁵³	-96.4 (-3.1)	0.0265	10.6
PTA-CH(<i>p</i> - $\text{C}_6\text{H}_4\text{OMe}$) OH ⁵³	-102.6 , -105.7 (-1.48 , -3.19)	0.0379	11.1

^aIn CDCl_3 . ^bPhosphine oxide chemical shift in parentheses.

PTA-Li even with dropwise addition of the imine at -78°C . The $^{31}\text{P}\{^1\text{H}\}$ NMR spectra of the crude products of 1 and 2 contained two singlets in ca. 1:1 ratio of *RS/SR:RR/SS* in CDCl_3 (-102.4 and -105.9 ppm for 1; -102.1 and -105.9 ppm for 2), Table 1. β -Aminophosphines 1 and 2 were isolated as diastereomeric mixtures in 3.5:1 (1) and 2.1:1 (2) ratio of *RS/SR:RR/SS* after a single recrystallization from THF and hexane (1:10). Repeated recrystallization from a 1:10 solution of THF/hexane resulted in the clean isolation of the *RS/SR* diastereomer of 1 (-102.4 ppm, 27%) and 2 (-102.1 ppm, 30%). Peruzzini and co-workers have previously reported the isolation of a single diastereomer for the oxide of PTA-CHPhOH by recrystallization.⁵⁵

The presence of $-\text{NHPh}$ moieties in 1–3 was confirmed by IR spectroscopy. A single IR absorption ($\nu_{\text{N-H}}$) was observed in the N–H stretching region of the infrared spectrum of 1 (3371 cm^{-1}), 2 (3360 cm^{-1}), and 3 (3323 cm^{-1}) indicating the presence of a secondary amine. The $\nu_{\text{N-H}}$ assignments were confirmed by H/D exchange. Reaction of 3 with D_2O in THF resulted in the disappearance of the absorbance at 3323 cm^{-1} and a new absorption at 2479 cm^{-1} corresponding to $\nu_{\text{N-D}}$.⁵⁸

The solid-state structures of compounds 1–3 were determined by single crystal X-ray diffraction. Crystals of 1 and 3 suitable for X-ray diffraction study were grown by slow evaporation of a 1:1 $\text{CH}_2\text{Cl}_2/\text{CH}_3\text{CN}$ solution of 1 or 3. Crystals of 2 were grown by slow evaporation of a 1:1 $\text{CH}_2\text{Cl}_2/\text{MeOH}$ solution of the single diastereomer of 2 (the stereochemistry of the racemate was determined to be $R_{\text{C}1}/S_{\text{C}7}$ and $S_{\text{C}1}/R_{\text{C}7}$). Thermal ellipsoid representations for 1 and 3 are depicted in Figures 1 and 2, respectively (see Supporting

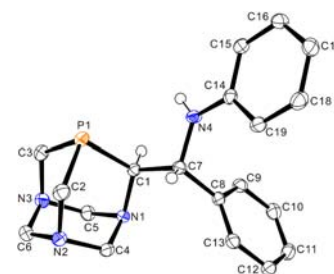


Figure 1. Thermal ellipsoid representation (50% probability) of PTA-CHPhNHPh (1) along with the atomic numbering scheme. Hydrogen atoms have been omitted except for those attached to N4 and stereocenters C1 and C7. Only the $S_{\text{C}1}/R_{\text{C}7}$ enantiomer is shown; however, both $S_{\text{C}1}/R_{\text{C}7}$ and $R_{\text{C}1}/S_{\text{C}7}$ are present in the structure.

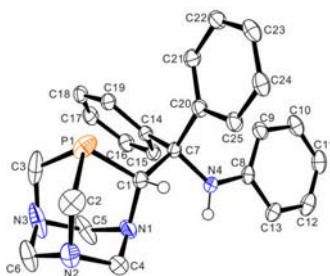


Figure 2. Thermal ellipsoid representation (50% probability) of PTA-CPh₂NHPh (**3**) with the atomic numbering scheme. Hydrogen atoms have been omitted except those attached to N4 and stereocenter C1. Only the R_{C1} enantiomer is shown; however, both enantiomers (S_{C1} and R_{C1}) are present in the structure.

Information for a thermal ellipsoid representation of **2**). All three structures contain both enantiomers in the respective unit cell: *RS/SR* for **1** and **2**, and *R/S* for **3**. The C7–C1–P1 bond angle in **1** and **2** are similar (110.19° and 111.83°, respectively) while this angle in **3** is significantly larger at 119.32°. This arises, presumably, from the increased steric bulk due to the additional phenyl ring on C7. Table 2 contains selected bond

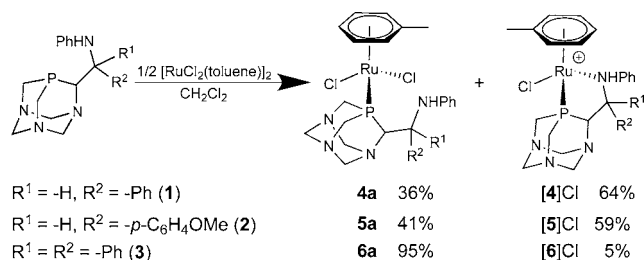
Table 2. Selected Bond Lengths (Å) and Angles (deg) for **1–3**

	1	2	3
P1–C1	1.880(2)	1.8830(12)	1.874(2)
P2–C2	1.860(2)	1.8662(12)	1.878(3)
P3–C3	1.862(2)	1.8608(13)	1.853(4)
N1–C1	1.480(2)	1.4767(16)	1.481(3)
C1–C7	1.548(3)	1.5460(15)	1.579(3)
N4–C7	1.460(2)	1.4487(16)	1.466(3)
N1–C1–C7	113.90(15)	111.47(9)	113.60(19)
C7–C1–P1	110.19(13)	111.83(8)	119.32(16)

lengths and angles. The amine proton in **2** forms a hydrogen bond with an oxygen atom of one of the two cocrystallized methanol molecules (N4...O2 = 2.9414(16) Å). Hydrogen bonding is also observed between the two methanol molecules (O2...O3 = 2.6942(18) Å) as well as between one of the lower-rim nitrogen atoms on the PTA cage and the hydroxyl group of methanol (O3...N3 = 2.7425(16) Å).⁵⁹

Ruthenium Arene Complexes. Ruthenium arene complexes of the β -aminophosphine ligands, PTA-CR¹R²NHPh, **1** (R¹ = H, R² = C₆H₅), **2** (R¹ = H, R² = *p*-C₆H₄OMe), and **3** (R¹ = R² = C₆H₅) were prepared by reaction of [(η^6 -C₆H₅CH₃)-RuCl(μ -Cl)]₂ with 2 equiv of the appropriate ligand (**1–3**) in dichloromethane, Scheme 3. The resulting air stable complexes **4–6** were isolated as orange solids in greater than 85% yield.

Scheme 3



The ruthenium arene complexes **4–6** are soluble in chloroform, dichloromethane, methanol, and acetonitrile but not soluble in diethyl ether and hexane. Complex **6** is not water-soluble at room temperature while complexes **4** and **5** are slightly water-soluble (*S*₂₅^o = 6 mg/mL for **4** and 5 mg/mL for **5**). As solids, compounds **4–6** are stable in air; however, solutions of **4–6** slowly decompose in air over the course of weeks turning dark brown/black.

As expected the β -aminophosphine ligands **1–3** are able to coordinate to the Ru center in either a monodentate (κ^1 -P) or bidentate (κ^2 -P,N) fashion with possible hemilabile behavior. κ^2 -P,N coordination of **1** or **2** to the ruthenium arene center results in an organometallic complex with three chiral centers: the ruthenium center and the two on the ligand. The hemilabile nature of the amine functionality allows for only two diastereomeric pairs to be observed in the ³¹P NMR spectrum. In polar solvents, such as water or methanol, complexes **4**, **5**, and **6** exist, predominantly, as the cationic [(η^6 -toluene)RuCl(κ^2 -P,N-PTA-CR¹R²NHPh)]Cl (**[4]Cl**, **[5]Cl**, and **[6]Cl**) with a chelating κ^2 -P,N coordination of **1**, **2**, and **3**, respectively, Table 3. In methanol only **4** is found to have any κ^1 -P

Table 3. Mole Fraction of κ^1 -P Coordination in **4a**, **5a**, **6a** in Various Solvents by ³¹P{¹H} NMR Spectroscopy at 25 °C

solvent	4a	5a	6a
CD ₃ OD	0.15	0.0	0.0
D ₂ O	0.0	0.0	0.0
CD ₃ CN	0.12 (0.16) ^a	0.09 (0.14) ^a	0.95 (0.96) ^a
CDCl ₃	0.36	0.41	0.95

^a50 °C.

coordination present in solution as measured by ³¹P NMR spectroscopy (~15%). In less polar solvents, such as CH₂Cl₂ or CHCl₃, **4–6** exist as equilibrium mixtures of monodentate (κ^1 -P) **4a–6a** and bidentate (κ^2 -P,N), **[4]Cl–[6]Cl**, coordination modes (Scheme 3 and Table 3). In CD₃CN **4** and **5** exist mainly as the κ^2 -P,N **[4]Cl** and **[5]Cl** whereas **6** is predominately found in the κ^1 -P coordination mode (**6a**). These results suggest hemilabile coordination of the nitrogen. Variable temperature NMR spectroscopy in CD₃OD or CDCl₃ between 0 and 50 °C revealed little variation in the coordination found for compounds **4–6**. In CD₃CN as the temperature was raised from 25 to 50 °C the mole fraction of κ^1 -P coordination increased slightly for **4** and **5**, while largely unchanged for **6** (Table 3).

The ³¹P{¹H} NMR spectrum of **6** in CDCl₃ (Figure 3a) contains two singlets at +0.6 and –31.1 ppm indicative of [(η^6 -toluene)RuCl₂(PTA-CPh₂NHPh)] (**6a**) and [(η^6 -toluene)-RuCl(PTA-CPh₂NHPh)]Cl (**[6]Cl**). Dissolving **6** in CD₃OD results in a single resonance at –0.4 ppm in the ³¹P{¹H} NMR spectrum indicating bidentate coordination of ligand **3** and dissociation of a chloride (Figure 3b). Addition of 10 equiv of NaCl to the CD₃OD solution of **6** results in the reappearance of a small singlet at –30.3 ppm indicating that **6a** and **[6]Cl** are indeed at equilibrium and that the nitrogen coordinates in a hemilabile fashion (Figure 3c). In CD₃CN **6** is mostly coordinated κ^1 -P with a large broad peak at –31.0 ppm and a small peak for κ^2 -P,N coordination at –0.5 ppm in the ³¹P{¹H} NMR spectrum. Ion exchange of **[6]Cl** to **[6]PF₆** resulted in exclusive bidentate P,N-coordination (single ³¹P{¹H} resonance at –0.7 ppm in CDCl₃, Figure 3d). Nitrogen coordination in **[6]PF₆** was confirmed by solid-state

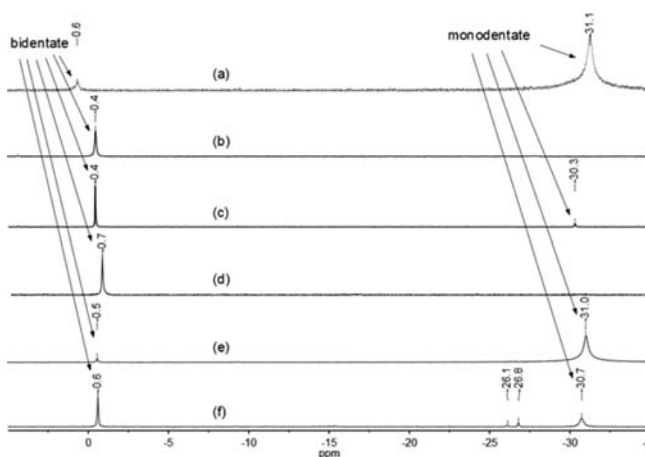


Figure 3. $^{31}\text{P}\{^1\text{H}\}$ NMR spectra: (a) $[\mathbf{6}]\text{Cl}$ and $\mathbf{6a}$ in CDCl_3 , (b) $[\mathbf{6}]\text{Cl}$ in CD_3OD , (c) $[\mathbf{6}]\text{Cl}$ and $\mathbf{6a}$ in $\text{CD}_3\text{OD} + 10$ equiv of NaCl , (d) $[\mathbf{6}]\text{PF}_6$ in CDCl_3 , (e) $[\mathbf{6}]\text{Cl}$ and $\mathbf{6a}$ in CD_3CN , (f) $[\mathbf{6}]\text{PF}_6$ and $\mathbf{6a}$ in CD_3CN .

IR spectroscopy. The ν_{NH} in $[\mathbf{6}]\text{PF}_6$ (3154 cm^{-1}) was found to be 169 cm^{-1} lower than the ν_{NH} in the free ligand $\mathbf{3}$ (3323 cm^{-1}) consistent with amine coordination to the metal center.⁶⁰ Dissolution of $[(\eta^6\text{-toluene})\text{RuCl}(\text{PTA-CPh}_2\text{NPh})]\text{PF}_6$ ($[\mathbf{6}]\text{PF}_6$) in a coordinating solvent, such as CD_3CN , reveals the hemilabile nature of the β -aminophosphine ligand. A mixture of monodentate (-30.7 ppm) and bidentate (-0.6 ppm) coordination is observed by $^{31}\text{P}\{^1\text{H}\}$ NMR spectroscopy along with two resonances at -26.1 and -26.8 , likely nitrile coordinated species, Figure 3f.

In CD_3OD only bidentate coordination is observed in the $^{31}\text{P}\{^1\text{H}\}$ NMR spectrum of $\mathbf{5}$ ($[\mathbf{5}]\text{Cl}$; -10.6 and -17.4 ppm , Figure 4b). Compound $\mathbf{4}$ in methanol contains $\sim 15\%$ of the κ^1 -

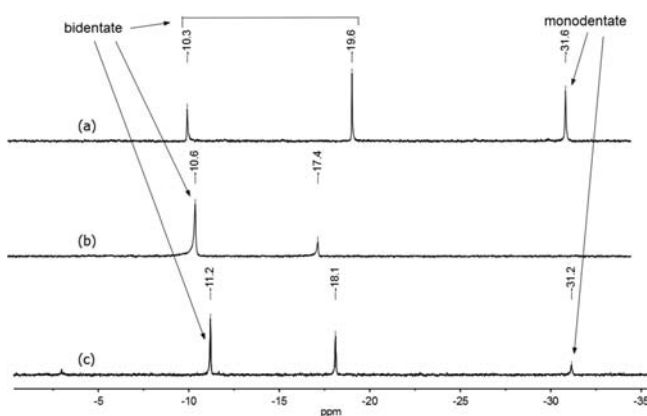


Figure 4. $^{31}\text{P}\{^1\text{H}\}$ NMR spectra: (a) $[\mathbf{5}]\text{Cl}$ and $\mathbf{5a}$ in CDCl_3 , (b) $[\mathbf{5}]\text{Cl}$ in CD_3OD , (c) $[\mathbf{5}]\text{Cl}$ and $\mathbf{5a}$ in CD_3CN .

P coordination mode ($[\mathbf{4}]\text{Cl}$; -10.5 and -17.7 ppm ; $\mathbf{4a}$; -30.4 ppm).⁵⁹ Redissolution of $[\mathbf{5}]\text{Cl}$ in chlorinated solvents (CD_2Cl_2 or CDCl_3) results in the appearance of an additional peak in the $^{31}\text{P}\{^1\text{H}\}$ NMR spectrum at -31.6 ppm for $\mathbf{5a}$ (Figure 4a) indicating both monodentate ($\mathbf{5a}$, -31.6 ppm) and bidentate ($[\mathbf{5}]\text{Cl}$, -10.3 and -19.6 ppm) coordination. Other ruthenium $\kappa^1\text{-P}$ complexes of PTA and derivatives have contained resonances in the -30 to -35 ppm region of the ^{31}P NMR spectrum.⁵³

Slow evaporation of a CH_3CN solution of complex $[\mathbf{5}]\text{Cl}$ or $[\mathbf{6}]\text{PF}_6$ over the course of a few days resulted in orange blocks suitable for single crystal X-ray diffraction. The $\kappa^2\text{-P,N}$ coordination in $[\mathbf{5}]\text{Cl}$ and $[\mathbf{6}]\text{PF}_6$ was confirmed by the X-ray diffraction analysis, Figures 5 and 6. The Ru(II) coordination sphere for $[\mathbf{5}]\text{Cl}$ and $[\mathbf{6}]\text{PF}_6$ each contain one η^6 -arene ring, one chloride, one phosphorus, and one nitrogen atoms. The Ru1– $\text{arene}_{\text{centroid}}$ for $[\mathbf{5}]\text{Cl}$ and $[\mathbf{6}]\text{PF}_6$ is 1.701 and 1.711 \AA , respectively. The Ru1–P1 distances for $[\mathbf{5}]\text{Cl}$ ($2.2833(7)\text{ \AA}$) and $[\mathbf{6}]\text{PF}_6$ ($2.2742(5)\text{ \AA}$) are slightly shorter than those observed for ruthenium arene complexes of $\kappa^1\text{-P}$ PTA derivatives ($2.3108(15)$ – $2.3294(11)\text{ \AA}$).⁵³ The Ru1–N4 distances in $[\mathbf{5}]\text{Cl}$ ($2.236(2)\text{ \AA}$) and $[\mathbf{6}]\text{PF}_6$ ($2.2206(15)\text{ \AA}$) are comparable to other β -aminophosphines complexes of ruthenium with $\kappa^2\text{-P,N}$ coordination and secondary amines (2.203 – 2.253 \AA).^{12,61} Although only one enantiomer $S_{\text{Ru}}S_{\text{C}_1}R_{\text{C}_7}$ and $S_{\text{Ru}}R_{\text{C}_1}$ is shown for $[\mathbf{5}]\text{Cl}$ (Figure 5) and $[\mathbf{6}]\text{PF}_6$ (Figure

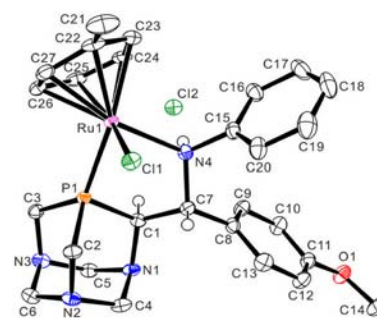


Figure 5. Thermal ellipsoid representation (50% probability) of $[\mathbf{5}]\text{Cl}$ with the atomic numbering scheme. Hydrogen atoms have been omitted except those bonded to the stereocenters or heteroatoms. Only the $S_{\text{Ru}}S_{\text{C}_1}R_{\text{C}_7}$ enantiomer is shown; however, both $S_{\text{Ru}}S_{\text{C}_1}R_{\text{C}_7}$ and $R_{\text{Ru}}R_{\text{C}_1}S_{\text{C}_7}$ are present in the structure. Selected bond lengths (\AA) and angles (deg): Ru1–N4 $2.236(2)$, Ru1–P1 $2.2833(7)$, Ru1–Cl1 $2.3979(8)$, Ru1– $\text{arene}_{\text{centroid}}$ 1.701 , N4–C7 $1.517(3)$, N4–Ru1–P1 $79.90(6)$, P1–Ru1–Cl1 $87.93(3)$, N4–Ru1–Cl1 $89.48(7)$.

6), both enantiomers are present in the unit cell (SSR/RRS for $[\mathbf{5}]\text{Cl}$; SR/RS for $[\mathbf{6}]\text{PF}_6$).⁶² The five-membered chelate ring

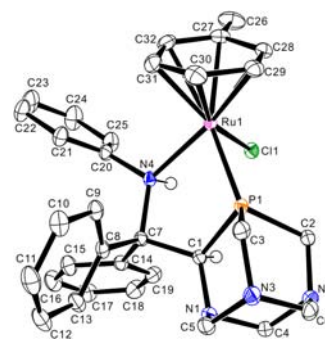
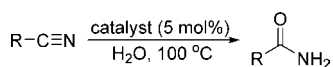


Figure 6. Thermal ellipsoid representation (50% probability) of the cationic portion of $[\mathbf{6}]\text{PF}_6$ with the atomic numbering scheme. Hydrogen atoms have been omitted except those bonded to the stereocenters or heteroatoms. The PF_6^- counterion has also been omitted for clarity. Only the $S_{\text{Ru}}R_{\text{C}_1}$ enantiomer is shown; however, both $S_{\text{Ru}}R_{\text{C}_1}$ and $R_{\text{Ru}}S_{\text{C}_1}$ are present in the structure. Selected bond lengths (\AA) and angles (deg): Ru1–N4 $2.2206(15)$, Ru1–P1 $2.2742(5)$, Ru1–Cl1 $2.4051(4)$, Ru1– $\text{arene}_{\text{centroid}}$ 1.711 , N4–C7 $1.559(2)$, N4–Ru1–P1 $79.31(4)$, P1–Ru1–Cl1 $85.083(16)$, N4–Ru1–Cl1 $80.30(4)$.

(Ru1–P1–C1–C7–N4) has a slightly twisted conformation, and the bite angle (N4–Ru1–P1) of the P,N chelate ring is 79.90(6)° and 79.31(4)° for [5]Cl or [6]PF₆, respectively. A weak hydrogen bond between Cl2 and the amine-N4 atoms was observed for [5]Cl (N4...Cl2 = 3.345(3) Å).

Aqueous Nitrile Hydration. While [RuCl₂(η⁶-arene)-(PTA)] was demonstrated as an efficient catalyst for aqueous nitrile hydration,⁵¹ we were intrigued to explore if such hydration efficiency could be retained or improved upon using the functionalized PTA derivatives, 1–3, as ligands. In particular, we envisioned that the hemilabile amine functionality could serve as a hydrogen-bond acceptor activating water and could also help promote dissociation of the product amide (at times considered the rate-determining step of nitrile hydration).²⁶ The structures of ruthenium arene complexes (*vide supra*) reveal that the pendant amine group on ligands 1, 2, and 3 is capable of binding the metal center and is also close enough to help activate water for nucleophilic attack. The catalytic hydration of benzonitrile to benzamide by [4]Cl, [5]Cl, and [6]Cl as well as other ruthenium complexes was evaluated. A typical catalytic experiment was carried out by mixing in air 5 mol % catalyst, 1 mmol nitrile, and 3 mL water in a culture tube at 100 °C (Scheme 4). The reaction was monitored by GC-MS at 7 and 24 h (Table 4).

Scheme 4

Table 4. Catalytic Hydration of Benzonitrile by Various Ru Compounds in Water in the Presence of Air^a

entry	catalyst	% conv ^b	TOF (h ⁻¹) ^c
1	[RuCl ₂ (η ⁶ -toluene)] ₂	0	0
2	RuCl ₃ ·3H ₂ O	(54)	0.45
3	[CpRu(PTA)(PPh ₃)Cl]	2(6)	0.06
4	[CpRu(PTA) ₂ Cl]	6(20)	0.17
5	[Cp* ₂ Ru(PTA) ₂ Cl]	24(57)	0.69
6	[IndRu(PTA)(PPh ₃)Cl]	29(77)	0.83
7	[RuCl ₂ (η ⁶ -toluene)(PTA)]	47(96)	1.3
8	[4]Cl	53(80)	1.5
9	[5]Cl	60(79)	1.7
10	[6]Cl	95(97)	2.7
11	RuCl ₂ PTA ₄ ⁵⁰	99	2.8 ^d

^aConditions: 1 mmol nitrile, 5 mol % cat., 3 mL H₂O, 100 °C, in air. ^bGC yields of amide after 7 h (24 h yield in parentheses). ^cTOF = mol product/(mol cat.-h) determined after 7 h. ^dTOF up to 30 h⁻¹ were observed for this catalyst.

Hydration did not proceed in the absence of a catalyst or in the presence of [RuCl₂(η⁶-toluene)] (Table 4, entry 1). RuCl₃·3H₂O showed a 54% conversion after 24 h (entry 2).⁶³ [CpRu(PTA)(PPh₃)Cl] and [CpRu(PTA)₂Cl] (Cp = η⁵-cyclopentadienyl) showed poor activity for the hydration of benzonitrile with conversions of 2–6% after 7 h and 6–20% after 24 h (Table 4, entries 3–4). It is not surprising that [CpRu(PTA)(PPh₃)Cl] and [CpRu(PTA)₂Cl] were not active, as it has been reported that CpRu phosphine complexes hydrate terminal alkynes in the presence of nitriles.^{64–66} The more electron-rich Cp*₂Ru(PTA)₂Cl complex (Cp* = η⁵-pentamethylcyclopentadienyl) exhibited improved activity compared to CpRu(PTA)₂Cl (entries 4–5). Cadierno and

co-workers reported higher performance with more sterically demanding and electron-rich arenes (C₆Me₆ > 1,3,5-C₆H₃Me₃ > *p*-cymene > C₆H₆) with a series of [RuCl₂(η⁶-arene)(PTA)] complexes.⁵¹ The indenyl complex [IndRu(PTA)(PPh₃)Cl] (Ind = η⁵-indenyl) exhibited the highest conversion (77%) and TOF (0.83 h⁻¹) among the cyclopentadienyl complexes (Table 4, entries 3–6). Presumably this is due to the indenyl effect, η⁵- to η³-rearrangement, facilitating nitrile coordination to ruthenium.

Complex [6]Cl (95%, TOF = 2.7 h⁻¹) was found to be much more active than [4]Cl (53%, TOF = 1.5 h⁻¹) or [5]Cl (60%, TOF = 1.7 h⁻¹) in the catalytic production of benzamide (Table 4, entries 8–10). The activity seems to correlate with the observation that 6 in acetonitrile is almost exclusively in the κ¹-P form (6a); however, 4 and 5 are observed mostly in the κ²-P,N form in acetonitrile and other polar solvents such as water and methanol. Ruthenium arene complexes with κ²-P,N coordination have been shown to be less active than similar κ¹-P coordinated complexes.³⁴ The more labile Ru–N bond in [6]Cl, allowing nitrile coordination to ruthenium, may be responsible for the increased activity. For comparison the κ¹-P coordinated complex [RuCl₂(η⁶-toluene)(PTA)] did not exhibit comparable efficiency (47%; Table 4, entry 7). Presumably, the lower efficiency was due to catalyst decomposition; a black oily precipitate was observed during and after hydration. Catalyst degradation was observed in [6]Cl catalyzed nitrile hydration with small amounts of both benzophenone and aniline observed by GC-MS. Catalyst decomposition was not observed, by GC-MS, for benzonitrile hydration by [4]Cl or [5]Cl. However, in all cases a black oily precipitate was observed following catalysis, unlike the clear solutions we observed in nitrile hydration catalyzed by [RuCl₂PTA₄].

Catalyst lifetime and activity were explored by looking at turnover number (TON) and turnover frequency (TOF)⁶⁷ for the hydration of benzonitrile to benzamide at various catalyst loadings from 5 mol % to 0.001 mol %, Table 5. Interestingly the TOF of the catalyst increased significantly as the catalyst loading was reduced. This is consistent with what we have previously reported for nitrile hydration catalyzed by [RuCl₂PTA₄].⁵⁰ TONs up to 97 000 were observed along

Table 5. Effect of Catalyst Loading on TON and TOF for Benzonitrile Hydration Catalyzed by [6]Cl or [6]PF₆^{a,59}

entry	catalyst (mol %)	time (h)	conv ^b	TON	TOF ^c (h ⁻¹)
1	5	7	95	19	2.7
2 ^d	5	7	78	16	2.2
3	1	7	74	74	10.6
4 ^d	1	7	44	44	6.3
5 ^e	1	7	92	92	13.1
6 ^f	1	7	89	89	12.7
7	1	12	94	94	7.8
8	1	24	98	98	4.1
9 ^g	1	24	73	73	3.0
10	0.1	100	97	970	9.7
11	0.01	160	56	5600	35
12	0.001	340	97	97 000	285

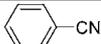
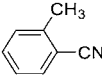
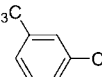
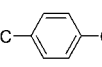
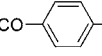
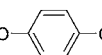
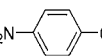
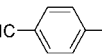
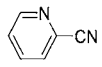
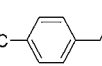
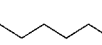
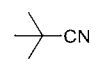
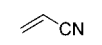
^aConditions: 1 mmol nitrile, 3 mL H₂O, 100 °C, in air. ^bDetermined by GC. ^cmol product/(mol catalyst-h). ^dReaction run with ~0.5 mL Hg. ^eReaction run with 10 mol % NaCl. ^fReaction run with 25 mol % NaCl. ^g[6]PF₆.

with TOF up to 285 h⁻¹ making [6]Cl an active and long-lived nitrile hydration catalyst, more active than the highly recyclable [RuCl₂PTA₄] where TON of up to 22 000 and TOF of up to 30 h⁻¹ were observed.⁵⁰ To test the effect of chloride we looked at the activity of [6]PF₆ (TOF = 3.0 h⁻¹, Table 5, entry 9) and found it to be slightly less active than [6]Cl (TOF = 4.1 h⁻¹, Table 5, entry 8). This difference in activity is ascribed to the difference in coordination of [6]Cl (>95% κ¹-P) and [6]PF₆ (~50:50 κ¹-P:κ²-P,N) in acetonitrile.⁵⁹ At 1 mol % catalyst a slight enhancement (TOF up to 13.1 h⁻¹) in rate was observed when 10 mol % NaCl was added to the reaction (Table 5, entry 5). When 25 mol % Cl⁻ was added, a slightly lower conversion and TOF was observed (12.7 h⁻¹ 89% at 7 h entry 6). The addition of mercury had a slight inhibitory effect on catalysis (Table 5, entries 2 and 4, with additional data available in Supporting Information). These mercury experiments are far from conclusive, but do suggest a combination of heterogeneous and homogeneous mechanisms.

Catalyst Scope. The catalytic activity of [6]Cl was further explored and extended to the hydration of various aromatic, aliphatic, and vinyl nitriles (Table 6). All nitriles, with the exception of acrylonitrile, were converted to their corresponding amides with 47–99% conversion in 24 h as determined by GC-MS (isolated yields ranged from 36% to 85%). Substituted benzonitriles were successfully converted to the corresponding amides with those containing electron-withdrawing groups (entries 7–9) obtained in better conversion compared to benzonitriles with electron-donating groups (entries 2–6). Hydration of *o*-tolunitrile (entry 2) was found to be less efficient compared to that of *m*- or *p*-tolunitrile (entries 3–4) attributed to the steric hindrance of *o*-tolunitriles. Hydration of heteroaromatics has been reported to be more challenging due to the strong coordinating ability of the heteroatom to the metal. Picolinamide can be obtained in a moderate conversion (47% after 24 h) by hydrating 2-cyanopyridine (entry 10). Aliphatic nitriles (entries 11–14) were also hydrated to the corresponding amides in 24 h. Transformation of 4-methylbenzyl cyanide to the amide reached a 93% conversion in 24 h (entry 11). Heptyl cyanide was converted to octamide in a moderate conversion (42% after 7 h, entry 12). The bulky pivalonitrile was converted into pivalamide with a 79% conversion after 24 h (entry 13). The hydration of acrylonitrile did not result in a clean reaction as evidenced by GC-MS analysis.⁵⁹

In summary, the insertion of imines into the C–Li bond of PTA-Li has provided access to a series of β-aminophosphine ligands (1–3). These ligands function as hemilabile ligands to ruthenium with both κ¹-P and κ²-P,N coordination modes observed depending on solvent and counterion. Presumably due to the presence of the hemilabile amine functionality a ruthenium arene complex of ligand 3 was a highly active catalyst for the hydration of nitriles in water with tolerance for air. Although some catalyst decomposition was observed during hydration, 6 showed excellent efficiency for aqueous nitrile hydration with tolerance toward a variety of functional groups and air. It is unclear, at this point, if the high activity is due to activation of water by the pendant amine or if the amine is helping push the product amide off of the metal center. As the hemilabile nature of ligand 3 appears important for catalytic hydration, studies are currently underway focused on the role of the pendant amine and the hemilabile nature of ligands 1–3.

Table 6. Hydration of Various Nitriles Catalyzed by [6]Cl^a

Entry	Substrate	Conv. ^b (%)	Yield ^c (%)	TOF ^d h ⁻¹
1		95(97)	85	2.7
2		31(64)	52	0.88
3		76(96)	83	2.2
4		70(94)	79	2.0
5		75(90)	74	2.1
6		67(83)	65	1.9
7		84(96)	76	2.4
8 ^e		98(99)	82	2.8
9		85(97)	79	2.4
10		24(47)	36	0.68
11		51(93)	81	1.5
12		42(62)	51	1.2
13		61(79)	66	1.7
14		^f	57	----

^aConditions: nitrile (1 mmol), [6]Cl (5 mol %), H₂O (3 mL), 100 °C, in air. ^bGC yields of amide after 7 h (24 h yield in parentheses). ^cIsolated by column chromatography. ^dTOF calculated using % conversion at 7 h. ^e0.2 mL DME was added to help with solubility. ^fThe hydration of acrylonitrile did not result in a clean reaction as evidenced by GC-MS analysis (see Supporting Information).

EXPERIMENTAL SECTION

Materials and Methods. Unless otherwise noted all manipulations were performed on a double-manifold Schlenk vacuum line under nitrogen or in a nitrogen-filled glovebox. Solvents were freshly distilled from standard drying reagents (Na/benzophenone for THF and hexanes; Mg/I₂ for methanol) or dried with activated molecular sieves and degassed with nitrogen, prior to use. *n*-Butyllithium, benzonitrile, *o*-tolunitrile, *m*-tolunitrile, *p*-tolunitrile, *p*-methoxybenzonitrile, *p*-cyanophenol, *p*-nitrobenzonitrile, *p*-bromobenzonitrile, *p*-cyanobenzaldehyde, 2-cyanopyridine, 4-methylbenzyl cyanide, heptyl cyanide, pivalonitrile, acrylonitrile, and deuterated NMR solvents were

obtained from commercial sources and used as received. Tetrakis-(hydroxymethyl)phosphonium chloride was obtained from Cytec and used without further purification. 1,3,5-Triaza-7-phosphaadamantane (PTA),⁶⁸ PTA-Li,⁵² *N*-benzylideneaniline (PhN=CHPh),⁶⁹ *N*-(4-methoxybenzylidene)aniline (PhN=CH(*p*-C₆H₄OCH₃)),⁶⁸ *N*-(diphenylmethylene)aniline (PhN=CPh₂),⁶⁸ and [(η⁶-C₆H₅CH₃)-RuCl₂]₂⁷⁰ were synthesized as reported in the literature. NMR spectra were recorded on a Varian NMR System 400 spectrometer with chemical shifts reported in ppm. ¹H and ¹³C NMR spectra were referenced to residual solvent relative to tetramethylsilane (TMS). Phosphorus chemical shifts are relative to an external reference of 85% H₃PO₄ in D₂O with positive values downfield of the reference. IR spectra were recorded on a Perkin-Elmer 2000 FT-IR spectrometer as a KBr pellet for solid samples. GC-MS analyses were obtained using a Varian CP 3800 GC (DB5 column) equipped with a Saturn 2200 MS and a CP 8410 autoinjector or an Agilent 7890A GC equipped with an Agilent 5975C inert MSD with triple axis detector and an Agilent 7693 autosampler. X-ray crystallographic data were collected at 100(±1) K on a Bruker APEX CCD diffractometer with Mo K α radiation (λ = 0.71073 Å) and a detector-to-crystal distance of 4.94 cm. Data collection was optimized utilizing the APEX 2 software with 0.5° rotation between frames. Data integration, correction for Lorentz and polarization effects, and final cell refinement were performed using SAINTPLUS and corrected for absorption using SADABS. The structures were solved by direct methods and refined using SHELXTL, version 6.10. All non-hydrogen atoms were refined anisotropically and hydrogen atoms placed in calculated positions. Crystallographic data and data collection parameters are listed in Table 2-S (see Supporting Information).

Caution! PTA-Li is a highly pyrophoric solid, igniting violently upon exposure to air.

Synthesis of PTA-CHPhNHPH (1). A suspension of PTA-Li (1.64 g, 10.0 mmol) in THF (40 mL) was cooled to -78 °C, and a THF solution (20 mL) of *N*-benzylideneaniline (1.83 g, 10.1 mmol) was added via cannula. The resulting mixture was kept at -78 °C for 30 min, after which the solution was slowly warmed to room temperature. After stirring for 1 h, an orange homogeneous solution formed. Following 2 h of stirring, distilled water (3 mL) was added to quench the reaction, and the solvent was removed under reduced pressure. The resulting residue was dissolved in water (30 mL) and extracted with dichloromethane (40 mL \times 4). The combined organic layers were dried with anhydrous potassium carbonate, filtered through Celite, and evaporated to dryness under reduced pressure to give a yellow oil. The yellow oil was taken up into THF (10 mL), followed by adding hexanes (120 mL) under nitrogen. After being placed in the freezer for 1 h, this mixture was filtered, washed with hexane (10 mL \times 3), and dried *in vacuo* to afford the desired product as a pale yellow powder (2.13 g, 63% yield) isolated as a mixture of diastereomers in a ~3.5:1 ratio of RS/SR:RR/SS. ¹H NMR (400 MHz, CDCl₃): δ 7.48 (d, J_{HH} = 7.2 Hz, 2H_{RR/SS}, Ar), 7.45 (d, J_{HH} = 7.2 Hz, 2H_{RS/SR}, Ar), 7.33 (t, J_{HH} = 7.2 Hz, 2H_{RR/SS}, Ar), 7.30 (t, J_{HH} = 7.2 Hz, 2H_{RS/SR}, Ar), 7.26–7.20 (m, 1H_{RS/SR} + 1H_{RR/SS}, Ar), 7.07 (t, J_{HH} = 7.6 Hz, 2H_{RS/SR}, Ar), 7.05 (t, J_{HH} = 7.6 Hz, 2H_{RR/SS}, Ar), 6.65 (t, J_{HH} = 7.6 Hz, 1H_{RR/SS}, Ar), 6.63 (t, J_{HH} = 7.6 Hz, 1H_{RS/SR}, Ar), 6.55 (d, J_{HH} = 7.6 Hz, 2H_{RR/SS}, Ar), 6.53 (d, J_{HH} = 7.6 Hz, 2H_{RS/SR}, Ar), 4.92–4.88 (br. m, NH), 4.88–4.86 (m, 1H_{RR/SS}, NCH₂N), 4.86–4.80 (m, 1H_{RS/SR}, PCHCHN), 4.74–4.61 (m, 2H_{RS/SR} + 2H_{RR/SS}, NCH₂N; 1H_{RR/SS}, PCHCHN), 4.60–4.42 (m, 4H_{RS/SR} + 3H_{RR/SS}, NCH₂N), 4.21–4.07 (m, 1H_{RS/SR} + 2H_{RR/SS}, PCH₂N), 4.09–3.99 (m, 1H_{RR/SS}, PCH₂N), 4.04–3.97 (m, 1H_{RS/SR}, PCHN), 3.94–3.85 (m, 1H_{RS/SR} + 1H_{RR/SS}, PCH₂N), 3.74–3.66 (m, 1H_{RS/SR}, PCH₂N), 3.65–3.60 (m, 1H_{RR/SS}, PCHN), 3.59–3.51 (m, 1H_{RS/SR}, PCH₂N). ¹³C{¹H} NMR (100 MHz, CDCl₃): 148.1 (s, Ar, RR/SS), 146.9 (s, Ar, RS/SR), 141.9 (d, ³J_{PC} = 1.5 Hz, Ar, RS/SR), 141.5 (d, ³J_{PC} = 2.2 Hz, Ar, RR/SS), 129.2 (s, Ar, RS/SR), 129.1 (s, Ar, RR/SS), 128.6 (s, Ar, RS/SR), 128.5 (s, Ar, RR/SS), 128.2 (d, ⁴J_{PC} = 3.7 Hz, Ar, RR/SS), 127.9 (s, Ar, RR/SS), 127.6 (s, Ar, RS/SR), 127.1 (d, ⁴J_{PC} = 2.3 Hz, Ar, RS/SR), 117.8 (s, Ar, RR/SS), 117.6 (s, Ar, RS/SR), 114.0 (s, Ar, RR/SS), 113.6 (s, Ar, RS/SR), 77.3 (s, NCH₂N, RS/SR), 76.1 (s, NCH₂N, RR/SS), 74.2 (d, ³J_{PC} = 3.0 Hz, NCH₂N, RS/SR), 73.7 (d, ³J_{PC} = 3.0 Hz, NCH₂N, RR/SS), 67.4 (d, ³J_{PC} = 3.7 Hz,

NCH₂N, RS/SR), 66.4 (d, ³J_{PC} = 3.0 Hz, NCH₂N, RR/SS), 64.4 (d, ¹J_{PC} = 21.7 Hz, PCHN, RS/SR), 64.3 (d, ¹J_{PC} = 19.5 Hz, PCHN, RR/SS), 59.0 (d, ²J_{PC} = 10.6 Hz, PCHCHN, RS/SR), 58.6 (d, ²J_{PC} = 14.9 Hz, PCHCHN, RR/SS), 51.8 (d, ¹J_{PC} = 20.2 Hz, PCH₂N, RS/SR), 51.0 (d, ¹J_{PC} = 20.9 Hz, PCH₂N, RR/SS), 50.7 (d, ¹J_{PC} = 20.2 Hz, PCH₂N, RR/SS), 47.5 (d, ¹J_{PC} = 24.6 Hz, PCH₂N, RR/SS), 47.1 (d, ¹J_{PC} = 24.6 Hz, PCH₂N, RS/SR). ³¹P{¹H} NMR (162 MHz, CDCl₃): δ -102.4 (s, RS/SR), -105.9 (s, minor). IR (KBr, cm⁻¹): 3371 (ν_{NH}). HRMS (ESI, CH₃OH) *m/z* calcd for C₁₉H₂₃N₄P: [M]⁺ 338.1660; found 338.1651. Crystals suitable for X-ray diffraction were obtained by slow evaporation of a 1:1 CH₂Cl₂/CH₃CN solution of **1**, resulting in colorless blocks over the course of a few days. RS/SR enantiomers were separated from the diastereomeric mixture by repeated recrystallization from THF/hexane (1:10) as a yellow powder (948 mg, 27% yield). The ¹H, ¹³C{¹H}, and ³¹P{¹H} NMR assignments and spectra of pure RS/SR isomer are included in the Supporting Information.

Synthesis of PTA-CH(*p*-C₆H₄OCH₃)NHPH (2). A suspension of PTA-Li (1.69 g, 10.4 mmol) in THF (40 mL) was cooled to -78 °C, and a THF solution (20 mL) of *N*-(4-methoxybenzylidene)aniline (2.23 g, 10.6 mmol) was added via cannula. The resulting mixture was kept at -78 °C for 30 min, after which the solution was slowly warmed to room temperature. After stirring for 1 h, an orange homogeneous solution formed. Following 2 h of stirring, distilled water (3 mL) was added to quench the reaction, and the solvent was removed under reduced pressure. The resulting residue was dissolved in water (30 mL) and extracted with dichloromethane (40 mL \times 4). The combined organic layers were dried with anhydrous potassium carbonate, filtered through Celite, and evaporated to dryness under reduced pressure to give a yellow oil. The yellow oil was taken up into THF (10 mL), followed by adding hexanes (120 mL) under nitrogen. After being placed in the freezer for 1 h, this mixture was filtered, washed with hexane (10 mL \times 3), and dried *in vacuo* to afford the desired product as a white powder (2.39 g, 62% yield) isolated as a mixture of diastereomers in a ~2.1:1 ratio of RS/SR:RR/SS. ¹H NMR (400 MHz, CDCl₃): δ 7.38 (d, J_{HH} = 8.4 Hz, 2H_{RR/SS}, Ar), 7.36 (d, J_{HH} = 8.4 Hz, 2H_{RS/SR}, Ar), 7.07 (t, J_{HH} = 7.2 Hz, 2H_{RS/SR}, Ar), 7.06 (t, J_{HH} = 7.2 Hz, 2H_{RR/SS}, Ar), 6.87 (d, J_{HH} = 8.4 Hz, 2H_{RR/SS}, Ar), 6.84 (d, J_{HH} = 8.4 Hz, 2H_{RS/SR}, Ar), 6.65 (t, J_{HH} = 7.6 Hz, 1H_{RR/SS}, Ar), 6.63 (t, J_{HH} = 8.4 Hz, 1H_{RS/SR}, Ar), 6.55 (d, J_{HH} = 8.8 Hz, 2H_{RR/SS}, Ar), 6.53 (d, J_{HH} = 10.4 Hz, 2H_{RS/SR}, Ar), 4.93–4.84 (br. m, NH), 4.87–4.83 (m, 1H_{RR/SS}, NCH₂N), 4.82–4.77 (m, 1H_{RS/SR}, PCHCHN), 4.68–4.62 (m, 1H_{RR/SS}, PCHCHN), 4.73–4.62 (m, 2H_{RS/SR} + 2H_{RR/SS}, NCH₂N), 4.60–4.42 (m, 4H_{RS/SR} + 3H_{RR/SS}, NCH₂N), 4.21–4.10 (m, 1H_{RS/SR} + 2H_{RR/SS}, PCH₂N), 4.09–3.99 (m, 1H_{RR/SS}, PCH₂N), 4.04–3.97 (m, 1H_{RS/SR}, PCHN), 3.94–3.85 (m, 1H_{RS/SR} + 1H_{RR/SS}, PCH₂N), 3.77 (s, 3H_{RR/SS}, OCH₃), 3.76 (s, 3H_{RS/SR}, OCH₃), 3.74–3.66 (m, 1H_{RS/SR}, PCH₂N), 3.65–3.60 (m, 1H_{RR/SS}, PCHN), 3.59–3.51 (m, 1H_{RS/SR}, PCH₂N). ¹³C{¹H} NMR (100 MHz, CDCl₃): δ 159.2 (s, Ar, RR/SS), 159.0 (s, Ar, RS/SR), 148.2 (s, Ar, RR/SS), 146.9 (s, Ar, RS/SR), 133.5 (d, ³J_{PC} = 2.3 Hz, Ar, RS/SR), 133.3 (d, ³J_{PC} = 3.0 Hz, Ar, RR/SS), 129.2 (d, ⁴J_{PC} = 3.0 Hz, Ar, RR/SS), 129.1 (s, Ar, RS/SR), 129.0 (s, Ar, RR/SS), 128.1 (d, ⁴J_{PC} = 2.3 Hz, Ar, RS/SR), 117.8 (s, Ar, RR/SS), 117.5 (s, Ar, RS/SR), 114.0 (s, Ar, RR/SS), 113.9 (s, Ar, RS/SR), 113.9 (s, Ar, RR/SS), 113.6 (s, Ar, RS/SR), 77.3 (s, NCH₂N, RS/SR), 76.0 (s, NCH₂N, RR/SS), 74.3 (d, ³J_{PC} = 2.3 Hz, NCH₂N, RS/SR), 74.2 (d, ³J_{PC} = 2.2 Hz, NCH₂N, RR/SS), 67.3 (d, ³J_{PC} = 3.0 Hz, NCH₂N, RS/SR), 66.4 (d, ³J_{PC} = 2.2 Hz, NCH₂N, RR/SS), 64.5 (d, ¹J_{PC} = 18.7 Hz, PCHN, RR/SS), 64.3 (d, ¹J_{PC} = 21.7 Hz, PCHN, RS/SR), 58.4 (d, ²J_{PC} = 10.4 Hz, PCHCHN, RS/SR), 57.9 (d, ²J_{PC} = 15.0 Hz, PCHCHN, RR/SS), 55.2 (s, OCH₃, RS/SR + RR/SS), 51.8 (d, ¹J_{PC} = 20.2 Hz, PCH₂N, RS/SR), 51.0 (d, ¹J_{PC} = 20.9 Hz, PCH₂N, RR/SS), 47.4 (d, ¹J_{PC} = 24.6 Hz, PCH₂N, RR/SS), 47.1 (d, ¹J_{PC} = 24.6 Hz, PCH₂N, RS/SR). ³¹P{¹H} NMR (162 MHz, CDCl₃): δ -102.1 (s, RS/SR), -105.9 (s, RR/SS). IR (KBr, cm⁻¹): 3360 (ν_{NH}). HRMS (ESI, CH₃OH) *m/z* calcd for C₂₀H₂₅N₄OP: [M]⁺ 368.1766; found 368.1766. RS/SR enantiomers were separated from the diastereomeric mixture by repeated recrystallizations from THF/hexane (1:10) as a yellow powder (1.10 g, 30% yield). The ¹H, ¹³C{¹H}, and ³¹P{¹H} NMR

assignments and spectra of pure *RS/SR* isomer are included in the Supporting Information. Colorless crystals suitable for X-ray diffraction were obtained as blocks by slow evaporation of a 1:1 $\text{CH}_2\text{Cl}_2/\text{CH}_3\text{OH}$ solution of PTA-CH(*p*- $\text{C}_6\text{H}_4\text{OCH}_3$)NHPPh (*RS/SR* enantiomers) over the course of a few days.

Synthesis of PTA-CPh₂NHPPh (3). A suspension of PTA-Li (1.64 g, 10.0 mmol) in THF (40 mL) was cooled to -78°C , and a THF solution (20 mL) of *N*-(diphenylmethylene)aniline (2.60 g, 10.1 mmol) was added via cannula. The resulting mixture was kept at -78°C for 30 min, after which the solution was slowly warmed to room temperature. After stirring for 1 h, an orange homogeneous solution formed. Following 2 h of stirring, distilled water (3 mL) was added to quench the reaction, and the solvent was removed under reduced pressure. The resulting residue was dissolved in water (30 mL) and extracted with dichloromethane (40 mL \times 4). The combined organic layers were dried with anhydrous potassium carbonate, filtered through Celite, and evaporated to dryness under reduced pressure to give a yellow oil. The yellow oily crude product was taken up into THF (10 mL), followed by adding hexanes (120 mL) under nitrogen. After being placed in the freezer for 1 h, this mixture was filtered, washed with hexane (10 mL \times 3), and dried *in vacuo* to afford the desired product as a pale yellow crystalline powder (3.18 g, 77% yield). ^1H NMR (400 MHz, CDCl_3): δ 7.85 (d, $J_{\text{HH}} = 8.0$ Hz, 2H, Ar), 7.77 (d, $J_{\text{HH}} = 7.2$ Hz, 2H, Ar), 7.45–7.38 (m, 3H, Ar), 7.33–7.29 (m, 2H, Ar), 7.25–7.22 (m, 1H, Ar), 6.89 (dd, $J_{\text{HH}} = 8.8$ and 7.6 Hz, 2H), 6.52 (t, $J_{\text{HH}} = 7.2$ Hz, 1H, Ar), 6.41 (br. s, 1H, NH), 6.23 (dd, $J_{\text{HH}} = 8.8$ and 1.2 Hz, 2H, Ar), 4.88, 4.69 (AB quartet, $J = 13.2$ Hz, 2H, NCH_2N), 4.50 (s, 1H, PCHN), 4.46, 4.33 (AB quartet, $J = 13.2$ Hz, 2H, NCH_2N), 4.08, 3.56 (AB quartet, $J = 13.6$ Hz, 2H, NCH_2N), 4.00 (td, $J = 14.0$ and 1.8 Hz, 1H, PCH_2N), 3.83–3.74 (m, 1H, PCH_2N), 3.53 (t, $J = 14.0$ Hz, 1H, PCH_2N), 3.43–3.35 (m, 1H, PCH_2N). $^{13}\text{C}\{^1\text{H}\}$ NMR (100 MHz, CDCl_3): δ 145.5 (d, $J_{\text{PC}} = 1.5$ Hz, Ar), 142.4 (d, $J_{\text{PC}} = 2.3$ Hz, Ar), 138.4 (s, Ar), 130.6 (d, $J_{\text{PC}} = 7.5$ Hz, Ar), 129.1 (s, Ar), 128.5 (s, Ar), 128.2 (s, Ar), 128.1 (s, Ar), 127.8 (s, Ar), 127.3 (s, Ar), 116.6 (s, Ar), 115.4 (s, Ar), 79.4 (s, NCH_2N), 74.6 (d, $J_{\text{PC}} = 2.3$ Hz, NCH_2N), 72.5 (d, $J_{\text{PC}} = 26.9$ Hz, PCHN), 67.2 (d, $J_{\text{PC}} = 11.3$ Hz, CPh₂NHPPh), 66.2 (d, $J_{\text{PC}} = 3.0$ Hz, NCH_2N), 53.4 (d, $J_{\text{PC}} = 20.2$ Hz, PCH_2N), 47.8 (d, $J_{\text{PC}} = 25.4$ Hz, PCH_2N). $^{31}\text{P}\{^1\text{H}\}$ NMR (162 MHz, CDCl_3): δ -97.7 (s). IR (KBr, cm^{-1}): 3323 (sharp, ν_{NH}). HRMS (ESI, CH_3OH) m/z calcd for $\text{C}_{25}\text{H}_{27}\text{N}_4\text{P}$: $[\text{M}]^+$ 414.1973; found 414.1981. Colorless crystals suitable for X-ray diffraction were obtained as blocks by slow evaporation of a mixed $\text{CH}_2\text{Cl}_2/\text{CH}_3\text{OH}$ solution of **3** over the course of a few days.

Synthesis of the Oxides of 1–3 (1a–3a). The phosphine oxides (**1a–3a**) were obtained quantitatively by the addition of 0.2 mmol 30% H_2O_2 to a 1 mL D_2O solution of **1–3** (0.1 mmol). $^{31}\text{P}\{^1\text{H}\}$ NMR (162 MHz, CDCl_3): δ **1a**, -2.9 (s), -5.7 (s); **2a**, -2.9 (s), -5.7 (s); **3a**, -1.5 (s).

Synthesis of $[(\eta^6\text{-C}_6\text{H}_5\text{CH}_3)\text{RuCl}(\kappa^2\text{-}(\text{P},\text{N})\text{PTA-CHPhNHPPh})\text{Cl}]$ ([4]Cl). $[(\eta^6\text{-C}_6\text{H}_5\text{CH}_3)\text{RuCl}(\mu\text{-Cl})_2]$ (106 mg, 0.2 mmol) and PTA-CHPhNHPPh (137 mg, 0.4 mmol) were stirred in CH_2Cl_2 (20 mL) overnight, during which time a homogeneous solution formed. The solution was filtered through Celite and evaporated to dryness under reduced pressure. The resulting residue was dissolved in minimum CH_2Cl_2 , and hexane was added until an orange precipitate was observed. The solution was placed in the freezer for one hour, and the precipitate was filtered, washed with hexane, and dried *in vacuo* to give a yellow orange solid (206 mg, 85% yield). ^1H NMR (400 MHz, CD_3OD): δ 7.72 (d, $J = 7$ Hz, 1H, Ar), 7.62 (d, $J = 6$ Hz, 1H, Ar), 7.45 (dd, $J = 11$ and 7 Hz, 1H, Ar), 7.29–7.04 (m, 6H, Ar), 7.04–6.95 (m, 1H, Ar), 5.93–5.84 (m, 1H, $\text{C}_6\text{H}_5\text{CH}_3$), 5.50–5.41 (m, 1H, $\text{C}_6\text{H}_5\text{CH}_3$), 5.22 (d, $J = 6$ Hz, 1H, $\text{C}_6\text{H}_5\text{CH}_3$), 5.20–5.11 (m, 1H, PCH_2N), 5.08 (d, $J = 6$ Hz, 1H, $\text{C}_6\text{H}_5\text{CH}_3$), 5.05–4.95 (m, 1H, PCHCHN), 4.84–4.75 (m, 2H PCH_2N ; 1H NCH_2N), 4.76–4.71 (m, 1H, $\text{C}_6\text{H}_5\text{CH}_3$), 4.69 (s, 1H, NCH_2N), 4.66–4.57 (m, 2H, NCH_2N), 4.38 (dd, $J = 19$, 11 Hz, 2H, NCH_2N ; 1H PCH_2N), 4.24 (d, $J = 10$ Hz, 1H, PCHN), 2.08 (apparent doublet, $J = 1$ Hz, 3H, $\text{C}_6\text{H}_5\text{CH}_3$). ^{13}C NMR (100 MHz, CD_3OD): δ 149.08 (s, Ar), 134.60–134.47 (m, Ar), 134.43 (s, Ar), 129.36 (s, Ar), 129.17–129.07 (m, Ar), 128.59 (m, Ar), 127.25 (s, Ar), 126.17 (s, Ar), 98.38 (d, $J_{\text{PC}} = 8$ Hz, $\text{C}_6\text{H}_5\text{CH}_3$), 93.26

(s, $\text{C}_6\text{H}_5\text{CH}_3$), 80.22 (d, $J_{\text{PC}} = 5$ Hz, PCHCHN), 79.82 (s, $\text{C}_6\text{H}_5\text{CH}_3$), 75.12 (d, $J_{\text{PC}} = 5$ Hz, NCH_2N), 72.64 (d, $J_{\text{PC}} = 8$ Hz, NCH_2N), 65.88 (d, $J_{\text{PC}} = 8$ Hz, NCH_2N), 65.47 (d, $J_{\text{PC}} = 8$ Hz, $\text{C}_6\text{H}_5\text{CH}_3$), 64.14 (d, $J_{\text{PC}} = 21$ Hz, PCHC), 51.66–51.44 (m, PCH_2N), 50.68 (d, $J_{\text{PC}} = 15$ Hz, PCH_2N), 17.63 (s, $\text{C}_6\text{H}_5\text{CH}_3$). $^{31}\text{P}\{^1\text{H}\}$ NMR (162 MHz, CD_3OD): δ -10.39 (s), -17.24 (s), -29.91 (s). ESI-MS (positive, CH_3OH): $m/z = 566.76$ for $[(\eta^6\text{-C}_6\text{H}_5\text{CH}_3)\text{RuCl}(\text{PTA-CHPhNHPPh})]^+$. HRMS (ESI, CH_3OH) m/z calcd for $\text{C}_{26}\text{H}_{31}\text{ClN}_4\text{PRu}$: $[\text{M} - \text{Cl}]^+$ 561.1051; found 561.1039.

Synthesis of $[(\eta^6\text{-C}_6\text{H}_5\text{CH}_3)\text{RuCl}(\kappa^2\text{-}(\text{P},\text{N})\text{PTA-CH}(\text{p-C}_6\text{H}_4\text{OCH}_3)\text{NHPPh})\text{Cl}]$ ([5]Cl). $[(\eta^6\text{-C}_6\text{H}_5\text{CH}_3)\text{RuCl}(\mu\text{-Cl})_2]$ (136 mg, 0.26 mmol) and PTA-CH(*p*- $\text{C}_6\text{H}_4\text{OCH}_3$)NHPPh (190 mg, 0.52 mmol) were stirred in CH_2Cl_2 (20 mL) overnight, during which time a homogeneous mixture formed. The solution was filtered through Celite, and the solvent was removed under reduced pressure. The residue was dissolved in minimum CH_2Cl_2 (~ 10 mL), and hexane (80 mL) was added to precipitate the product. The precipitate was filtered and washed with hexane (5 mL \times 2) to give an orange solid (280 mg, 89% yield). ^1H NMR (400 MHz, CD_3OD): 7.72 (d, 1H, $J_{\text{HH}} = 8$ Hz, Ar), 7.60–7.48 (m, 1H, Ar), 7.42 (t, 1H, $J_{\text{HH}} = 8$ Hz, Ar), 7.28–6.98 (m, 6H, Ar), 5.98–5.88 (m, 1H, $\text{C}_6\text{H}_5\text{CH}_3$), 5.50 (t, 1H, $J_{\text{HH}} = 4.0$ Hz, $\text{C}_6\text{H}_5\text{CH}_3$), 5.30–5.10 (m, 2H, $\text{C}_6\text{H}_5\text{CH}_3$), 5.05 (d, 1H, $J = 8$ Hz, $\text{C}_6\text{H}_5\text{CH}_3$), 5.00–4.69 (m, 3H, NCH_2N ; 1H, PCHCHN; 3H, PCH_2N), 4.59 (d, 2H, $J = 12$ Hz, NCH_2N), 4.43–4.27 (m, 1H, PCHN; 1H, PCH_2N), 4.22 (d, 1H, $J = 12$ Hz, NCH_2N), 3.33 (3H, OCH_3), 2.07 (s, 3H, $\text{C}_6\text{H}_5\text{CH}_3$). $^{13}\text{C}\{^1\text{H}\}$ NMR (100 MHz, CD_3OD): δ 150.5 (s, Ar), 136.0 (d, $J_{\text{PC}} = 12$ Hz, Ar), 130.6 (d, $J_{\text{PC}} = 12$ Hz, Ar), 130.0 (s, Ar), 129.9 (s, Ar), 128.7 (s, Ar), 127.5 (s, Ar), 122.1 (s, Ar), 121.8 (s, Ar), 111.6 (d, $J_{\text{PC}} = 4.5$ Hz, $\text{C}_6\text{H}_5\text{CH}_3$), 99.9 (d, $J_{\text{PC}} = 9.0$ Hz, $\text{C}_6\text{H}_5\text{CH}_3$), 94.6 (d, $J_{\text{PC}} = 2.2$ Hz, $\text{C}_6\text{H}_5\text{CH}_3$), 81.7 (s, $\text{C}_6\text{H}_5\text{CH}_3$), 81.6 (s, $\text{C}_6\text{H}_5\text{CH}_3$), 81.2 (s, $\text{C}_6\text{H}_5\text{CH}_3$), 76.6 (d, $J_{\text{PC}} = 4.5$ Hz, NCH_2N), 74.0 (d, $J_{\text{PC}} = 7.5$ Hz, NCH_2N), 67.3 (d, $J_{\text{PC}} = 7.4$ Hz, NCH_2N), 66.8 (d, $J_{\text{PC}} = 8.1$ Hz, PCHCHN), 65.6 (d, $J_{\text{PC}} = 21.7$ Hz, PCHN), 52.9 (d, $J_{\text{PC}} = 12.7$ Hz, PCH_2N), 52.1 (d, $J_{\text{PC}} = 14.3$ Hz, PCH_2N), 19.2 (s, $\text{C}_6\text{H}_5\text{CH}_3$). $^{31}\text{P}\{^1\text{H}\}$ NMR (162 MHz, CD_3OD): δ -10.6 (s), -17.4 (s). ESI-MS (positive, CH_3OH): $m/z = 597.42$ for $[(\eta^6\text{-C}_6\text{H}_5\text{CH}_3)\text{RuCl}(\text{PTA-CH}(\text{p-C}_6\text{H}_4\text{OCH}_3)\text{NHPPh})]^+$. HRMS (ESI, MeOH) m/z calcd for $\text{C}_{27}\text{H}_{33}\text{ClN}_4\text{OPRu}$: $[\text{M} - \text{Cl}]^+$ 591.1157; found 591.1141. Orange crystals suitable for X-ray diffraction were obtained as plates by slow evaporation of a MeOH solution of the complex over the course of a few days.

Synthesis of $[(\eta^6\text{-C}_6\text{H}_5\text{CH}_3)\text{RuCl}(\kappa^2\text{-}(\text{P},\text{N})\text{PTA-CPh}_2\text{NHPPh})\text{Cl}]$ ([6]Cl). $[(\eta^6\text{-C}_6\text{H}_5\text{CH}_3)\text{RuCl}(\mu\text{-Cl})_2]$ (137 mg, 0.25 mmol) and PTA-CPh₂NHPPh (211 mg, 0.51 mmol) were stirred in CH_2Cl_2 (20 mL) overnight, during which time a homogeneous mixture formed. The solution was filtered through Celite, and the solvent was removed under reduced pressure. The residue was dissolved in minimum of CH_2Cl_2 (~ 10 mL), and hexane (80 mL) was added to precipitate the product. The precipitate was filtered and washed with hexane (5 mL \times 2) to give an orange solid (306 mg, 90% yield). ^1H and ^{13}C NMR spectra were obtained at 55°C due to the slightly broadening spectrum observed at room temperature. ^1H NMR (400 MHz, CD_3OD , 55°C): δ 8.68 (d, 1H, $J_{\text{HH}} = 8.4$ Hz, Ar), 7.86 (t, 1H, $J_{\text{HH}} = 7.8$ Hz, Ar), 7.61 (t, 2H, $J_{\text{HH}} = 7.4$ Hz, Ar), 7.33–7.12 (m, 8H, Ar), 6.92 (m, 2H, Ar), 6.76 (d, 1H, $J_{\text{HH}} = 8.0$ Hz, Ar), 6.40 (d, 1H, $J_{\text{HH}} = 7.6$ Hz, Ar), 6.14–6.08 (m, 1H, $\text{C}_6\text{H}_5\text{CH}_3$), 6.00 (t, 1H, $J = 5.2$ Hz, $\text{C}_6\text{H}_5\text{CH}_3$), 5.60 (t, 1H, $J = 5.6$ Hz, $\text{C}_6\text{H}_5\text{CH}_3$), 5.35 (d, 1H, $J = 6.0$ Hz, $\text{C}_6\text{H}_5\text{CH}_3$), 5.10 (d, 1H, $J = 6.0$ Hz, $\text{C}_6\text{H}_5\text{CH}_3$), 5.01 (d, $J = 10.8$ Hz, 1H, PCHN), 4.99 (d, $J = 15.2$ Hz, 1H, PCH_2N), 4.82 (d, $J = 13.2$ Hz, 1H, NCH_2N), 4.71–4.63 (m, 2H, PCH_2N ; 2H, NCH_2N), 4.46 (d, $J = 13.2$ Hz, 1H, NCH_2N), 4.37 (d, $J = 15.2$ Hz, 1H, PCH_2N), 3.88 (d, $J = 13.6$ Hz, 1H, NCH_2N), 2.54 (d, $J = 14.0$ Hz, 1H, NCH_2N), 2.00 (s, 3H, $\text{C}_6\text{H}_5\text{CH}_3$). $^{13}\text{C}\{^1\text{H}\}$ NMR (100 MHz, CD_3OD): δ 150.8 (d, $J_{\text{PC}} = 1.5$ Hz, Ar), 139.0 (s, Ar), 139.0 (s, Ar), 137.8 (s, Ar), 134.5 (s, Ar), 131.5 (s, Ar), 131.0 (s, Ar), 130.8 (s, Ar), 130.5 (s, Ar), 130.4 (s, Ar), 130.4 (s, Ar), 129.5 (s, Ar), 128.6 (s, Ar), 125.0 (s, Ar), 124.2 (s, Ar), 113.5 (d, $J_{\text{PC}} = 5.9$ Hz, $\text{C}_6\text{H}_5\text{CH}_3$), 101.3 (d, $J_{\text{PC}} = 8.2$ Hz, $\text{C}_6\text{H}_5\text{CH}_3$), 93.6 (d, $J_{\text{PC}} = 1.5$ Hz, $\text{C}_6\text{H}_5\text{CH}_3$), 82.8 (s, $\text{C}_6\text{H}_5\text{CH}_3$), 82.4 (s, $\text{C}_6\text{H}_5\text{CH}_3$), 82.0 (s, $\text{C}_6\text{H}_5\text{CH}_3$), 79.0 (d, $J_{\text{PC}} = 1.9$ Hz, NCH_2N), 77.9 (d, $J_{\text{PC}} = 3.7$ Hz, CPh₂), 74.7 (d, $J_{\text{PC}} = 4.5$ Hz, NCH_2N), 67.3 (d, $J_{\text{PC}} =$

10.5 Hz, NCH₂N), 67.0 (d, J_{PC} = 20.9 Hz, PCHN), 54.3 (d, J_{PC} = 18.0 Hz, PCH₂N), 52.0 (d, J_{PC} = 12.0 Hz, PCH₂N), 19.2 (s, C₆H₅CH₃). ³¹P{¹H} NMR (162 MHz, CDCl₃): δ 0.6 (s, minor), -16.4 (s, minor), -30.6 (s, major). ³¹P{¹H} NMR (162 MHz, CD₃OD): δ -0.4 (s). IR (KBr, cm⁻¹): 3308 (sharp, ν_{NH}). ESI-MS (positive, CH₃OH): m/z = 643.23 for [(η⁶-C₆H₅CH₃)RuCl(PTA-CPh₂NHPh)]⁺. HRMS (ESI, MeOH) m/z calcd for C₃₂H₃₅ClN₄PRu: [M - Cl]⁺ 637.1364; found 637.1378.

Synthesis of [(η⁶-C₆H₅CH₃)RuCl(κ²-(P,N)PTA-CPh₂NHPh)]PF₆ ([6]PF₆). [(η⁶-C₆H₅CH₃)RuCl₂(PTA-CPh₂NHPh)] (342 mg, 0.5 mmol) and potassium hexafluorophosphate (95 mg, 0.51 mmol) were stirred in CH₂Cl₂ (20 mL) for two days. The solution was filtered through Celite to remove KCl, and the solvent was removed under reduced pressure. The residue was dissolved in a minimum of CH₂Cl₂ (~10 mL), and hexane (80 mL) was added to precipitate the product. The precipitate was filtered and washed with hexane (5 mL × 2) to give a yellow-orange solid (329 mg, 86% yield). ¹H and ¹³C{¹H} NMR data are identical to [6]Cl in CD₃OD. ³¹P{¹H} NMR (162 MHz, CDCl₃): δ -0.7 (s), -143.6 (sept, ¹J_{PF} = 714 Hz, PF₆⁻). IR (KBr, cm⁻¹): 3154 (sharp, ν_{NH}), 843 (strong, ν_{PF}). ESI-MS (positive, CH₃OH): m/z = 643.50 for [(η⁶-C₆H₅CH₃)RuCl(PTA-CPh₂NHPh)]⁺. Orange crystals suitable for X-ray diffraction were obtained as plates by slow evaporation of a MeOH solution of the complex over the course of a few days.

General Procedure for Nitrile Hydration Reactions. Under air, the corresponding nitrile (1 mmol), 3 mL of water, and 5 mol % ruthenium catalyst were introduced into a Teflon-sealed screw-cap culture tube, and the reaction mixture was stirred at 100 °C. Aliquots were taken from the hot solution and extracted with CH₂Cl₂ (3 × 2 mL) at 7 and 24 h, and reaction progress was measured by GC-MS. At the end of 7 or 24 h the solvent was removed under reduced pressure and the crude product purified by column chromatography over silica gel with ethyl acetate as eluent. The identity of the resulting amides was assessed by comparison of their ¹H and ¹³C{¹H} NMR spectroscopic data with those reported in the literature. The retention time/fragmentation observed by GC-MS was also compared to that of an authentic sample.

■ ASSOCIATED CONTENT

● Supporting Information

Detailed procedures for separation of the diastereomers of **1** and **2**, additional catalytic results, crystallographic details (PDF and CIF), and NMR spectra of all compounds. This material is available free of charge via the Internet at <http://pubs.acs.org>.

■ AUTHOR INFORMATION

Corresponding Author

*E-mail: Frost@unr.edu.

Present Address

†Concordia College at Moorhead, 334F Ivers, Moorhead, MN, 56562.

Notes

The authors declare no competing financial interest.

■ ACKNOWLEDGMENTS

The authors thank the National Science Foundation CAREER program (CHE-0645365) and the donors of the American Chemical Society Petroleum Research Fund (PRF 43574-G3) for support. K.E. thanks the NSF-REU program (CHE-0552816) for summer support. The NSF is also acknowledged for the X-ray and NMR facilities at UNR (CHE-0226402 and CHE-0521191).

■ REFERENCES

(1) Weng, Z.; Teo, S.; Hor, T. S. A. *Acc. Chem. Res.* **2007**, *40*, 676–684.

(2) Braunstein, P.; Naud, F. *Angew. Chem., Int. Ed.* **2001**, *40*, 680–699.

(3) Amoroso, D.; Graham, T. W.; Guo, R.; Tsang, C.-W.; Abdur-Rashid, K. *Aldrichimica Acta* **2008**, *41*, 15–26.

(4) Slone, C. S.; Weinberger, D. A.; Mirkin, C. A. *Prog. Inorg. Chem.* **1999**, *48*, 233–350.

(5) Atkinson, R. C. J.; Gibson, V. C.; Long, N. J. *Chem. Soc. Rev.* **2004**, *33*, 313–328.

(6) Bader, A.; Lindner, E. *Coord. Chem. Rev.* **1991**, *108*, 27–110.

(7) Jutzi, P.; Siemeling, U. *J. Organomet. Chem.* **1995**, *500*, 175–185.

(8) Braunstein, P. *J. Organomet. Chem.* **2004**, *689*, 3953–3967.

(9) Faller, J. W.; Milheiro, S. C.; Parr, J. *J. Organomet. Chem.* **2008**, *693*, 1478–1493.

(10) Lindner, R.; van den Bosch, B.; Lutz, M.; Reek, J. N. H.; van der Vlugt, J. I. *Organometallics* **2011**, *30*, 499–510.

(11) Kwong, F. Y.; Chan, A. S. C. *Synlett* **2008**, *10*, 1440–1448.

(12) Abdur-Rashid, K.; Guo, R.; Lough, A. J.; Morris, R. H. *Adv. Synth. Catal.* **2005**, *347*, 571–579.

(13) Guo, R.; Morris, R. H.; Song, D. *J. Am. Chem. Soc.* **2005**, *127*, 516–517.

(14) Guo, R.; Lough, A. J.; Morris, R. H.; Song, D. *Organometallics* **2004**, *23*, 5524–5529.

(15) Hounjet, L. J.; Bierenstiel, M.; Ferguson, M. J.; McDonald, R.; Cowie, M. *Inorg. Chem.* **2010**, *49*, 4288–4300.

(16) Braunstein, P.; Graiff, C.; Naud, F.; Pfaltz, A.; Tiripicchio, A. *Inorg. Chem.* **2000**, *39*, 4468–4475.

(17) Yang, H.; Alvarez-Gressier, M.; Lugan, N.; Mathieu, R. *Organometallics* **1997**, *16*, 1401–1409.

(18) Bacchi, A.; Balordi, M.; Cammi, R.; Elviri, L.; Pelizzi, C.; Picchioni, F.; Verdolino, V.; Goubitz, K.; Peschar, R.; Pelagatti, P. *Eur. J. Inorg. Chem.* **2008**, 4462–4473.

(19) Andrieu, J.; Camus, J.-M.; Richard, P.; Poli, R.; Gonsalvi, L.; Vizza, F.; Peruzzini, M. *Eur. J. Inorg. Chem.* **2006**, 51–61.

(20) Moreno, M. A.; Haukka, M.; Jääskeläinen, S.; Vuoti, S.; Pursiainen, J.; Pakkanen, T. A. *J. Organomet. Chem.* **2005**, *690*, 3803–3814.

(21) Drommi, D.; Nicolò, F.; Arena, C. G.; Bruno, G.; Faraone, F.; Gobetto, R. *Inorg. Chim. Acta* **1994**, *221*, 109–116.

(22) Komuro, T.; Begum, R.; Ono, R.; Tobita, H. *Dalton Trans.* **2011**, *40*, 2348–2357.

(23) Jiménez, M. V.; Pérez-Torrente, J. J.; Bartolomé, M. I.; Gierz, V.; Lahoz, F. J.; Oro, L. A. *Organometallics* **2008**, *27*, 224–234.

(24) Gareau, D.; Sui-Seng, C.; Groux, L. F.; Brisse, F.; Zargarian, D. *Organometallics* **2005**, *24*, 4003–4013.

(25) Thompson, S. M.; Stöhr, F.; Sturmayer, D.; Kickelbick, G.; Schubert, U. *J. Organomet. Chem.* **2003**, *686*, 183–191.

(26) Ahmed, T. J.; Knapp, S. M. M.; Tyler, D. R. *Coord. Chem. Rev.* **2011**, *255*, 949–974.

(27) Kukushkin, V. Y.; Pombeiro, A. J. L. *Inorg. Chim. Acta* **2005**, *358*, 1–21.

(28) Kukushkin, V. Y.; Pombeiro, A. J. L. *Chem. Rev.* **2002**, *102*, 1771–1802.

(29) Michelin, R. A.; Mozzon, M.; Bertani, R. *Coord. Chem. Rev.* **1996**, *147*, 299–338.

(30) Breno, K. L.; Ahmed, T. J.; Pluth, M. D.; Balzarek, C.; Tyler, D. R. *Coord. Chem. Rev.* **2006**, *250*, 1141.

(31) (a) Breno, K. L.; Pluth, M. D.; Tyler, D. R. *Organometallics* **2003**, *22*, 1203. (b) Breno, K. L.; Pluth, M. D.; Landorf, C. W.; Tyler, D. R. *Organometallics* **2004**, *23*, 1738.

(32) Oshiki, T.; Yamashita, H.; Sawada, K.; Utsunomiya, M.; Takahashi, K.; Takai, K. *Organometallics* **2005**, *24*, 6287.

(33) Ghaffar, T.; Parkins, A. W. *Tetrahedron Lett.* **1995**, *36*, 8657.

(34) García-Álvarez, R.; Diez, J.; Crochet, P.; Cadierno, V. *Organometallics* **2010**, *29*, 3955–3965.

(35) García-Garrido, S. E.; Francos, J.; Cadierno, V.; Basset, J.-M.; Polshettiwar, V. *ChemSusChem* **2011**, *4*, 104–111.

(36) Cavarzan, A.; Scarso, A.; Strukul, G. *Green Chem.* **2010**, *12*, 790–794.

- (37) Ashraf, S. M.; Berger, I.; Nazarov, A. A.; Hartinger, C. G.; Koroteev, M. P.; Nifant'ev, E. E.; Keppler, B. K. *Chem. Biodiversity* **2008**, *5*, 1640–1644.
- (38) Ashraf, S. M.; Kandioller, W.; Mendoza-Ferri, M.-G.; Nazarov, A. A.; Hartinger, C. G.; Keppler, B. K. *Chem. Biodiversity* **2008**, *5*, 2060–2066.
- (39) Cadierno, V.; Díez, J.; Francos, J.; Gimeno, J. *Chem.—Eur. J.* **2010**, *16*, 9808–9817.
- (40) Knapp, S. M. M.; Sherbow, S. J.; Julitte, J. J.; Tyler, D. R. *Organometallics* **2012**, *31*, 2941–2944.
- (41) For example see: (a) Scolari, C.; Bergamo, A.; Brescacin, L.; Delfino, R.; Cocchietto, M.; Laurenczy, G.; Geldbach, T. J.; Sava, G.; Dyson, P. J. *J. Med. Chem.* **2005**, *48*, 4161–4171. (b) Ang, W. H.; Daldini, E.; Scolari, C.; Scopelliti, R.; Juillerat-Jeannerat, L.; Dyson, P. J. *Inorg. Chem.* **2006**, *45*, 9006–9013. (c) Allardyce, C. S.; Dyson, P. J.; Ellis, D. J.; Heath, S. L. *Chem. Commun.* **2001**, 1396–1397. (d) Scolari, C.; Geldbach, T. J.; Rochat, S.; Dorcier, A.; Gossens, C.; Bergamo, A.; Cocchietto, M.; Tavernelli, L.; Sava, G.; Rothlisberger, U.; Dyson, P. J. *Organometallics* **2006**, *25*, 756–765. (e) Ang, W. H.; Daldini, E.; Juillerat-Jeannerat, L.; Dyson, P. J. *Inorg. Chem.* **2007**, *46*, 9048–9050.
- (42) For reviews, see: (a) Phillips, A. D.; Gonsalvi, L.; Romerosa, A.; Vizza, F.; Peruzzini, M. *Coord. Chem. Rev.* **2004**, *248*, 955–993. (b) Bravo, J.; Bolano, S.; Gonsalvi, L.; Peruzzini, M. *Coord. Chem. Rev.* **2010**, *254*, 555–607.
- (43) Dyson, P. J.; Ellis, D. J.; Laurenczy, G. *Adv. Synth. Catal.* **2003**, *345*, 211–215.
- (44) Bosquain, S. S.; Dorcier, A.; Dyson, P. J.; Erlandsson, M.; Gonsalvi, L.; Laurenczy, G.; Peruzzini, M. *Appl. Organometal. Chem.* **2007**, *21*, 947–951.
- (45) Mebi, C. A.; Frost, B. J. *Organometallics* **2005**, *24*, 2339–2346.
- (46) Mebi, C. A.; Nair, R. P.; Frost, B. J. *Organometallics* **2007**, *26*, 429–438.
- (47) Nair, R. P.; Kim, T. H.; Frost, B. J. *Organometallics* **2009**, *28*, 4681–4688.
- (48) Nair, R. P.; Pineda-Lanorio, J. A.; Frost, B. J. *Inorg. Chim. Acta* **2012**, *380*, 96–103.
- (49) Legrand, F.-X.; Hapiot, F.; Tilloy, S.; Guerriero, A.; Peruzzini, M.; Gonsalvi, L.; Monflier, E. *Appl. Catal., A* **2009**, *362*, 62–66.
- (50) Lee, W.-C.; Frost, B. J. *Green Chem.* **2012**, *14*, 62–66.
- (51) Cadierno, V.; Francos, J.; Gimeno, J. *Chem.—Eur. J.* **2008**, *14*, 6601–6605.
- (52) Wong, G. W.; Harkreader, J. L.; Mebi, C. A.; Frost, B. J. *Inorg. Chem.* **2006**, *45*, 6748–6755.
- (53) Wong, G. W.; Lee, W.-C.; Frost, B. J. *Inorg. Chem.* **2008**, *47*, 612–620.
- (54) Huang, R.; Frost, B. J. *Inorg. Chem.* **2007**, *46*, 10962–10964.
- (55) Erlandsson, M.; Gonsalvi, L.; Peruzzini, M. *Inorg. Chem.* **2008**, *47*, 8–10.
- (56) Guerriero, A.; Erlandsson, M.; Ienco, A.; Krogstad, D. A.; Peruzzini, M.; Reginato, G.; Gonsalvi, L. *Organometallics* **2011**, *30*, 1874–1884.
- (57) Krogstad, D. A.; Guerriero, A.; Ienco, A.; Manca, G.; Peruzzini, M.; Reginato, G.; Gonsalvi, L. *Organometallics* **2011**, *30*, 6292–6302.
- (58) The predicted $\nu_{(\text{N-D})}$ based on a Hooke's law calculation is 2426 cm^{-1} .
- (59) See Supporting Information for further details.
- (60) Andrieu, J.; Richard, P.; Camus, J.-M.; Poli, R. *Inorg. Chem.* **2002**, *41*, 3876–3885.
- (61) (a) Morris, R.; Habtemariam, A.; Guo, Z.; Parsons, S.; Sadler, P. *J. Inorg. Chim. Acta* **2002**, *339*, 551–559. (b) Rahman, M. S.; Prince, P. D.; Steed, J. W.; Hii, K. K. *Organometallics* **2002**, *21*, 4927–4933. (c) Ito, M.; Osaku, A.; Kobayashi, C.; Shiibashi, A.; Ikariya, T. *Organometallics* **2009**, *28*, 390–393.
- (62) The chirality at ruthenium is determined by the ligand priority $\text{Cl1} > \text{P1} > \text{N4} > \text{arene ring}$.
- (63) Benzonitrile hydration by 2 mol % RuCl_3 was previously reported to yield 28% benzamide after 3 h at 130 °C. Kazuya Yamaguchi, K.; Matsushita, M.; Mizuno, N. *Angew. Chem.* **2004**, *116*, 1602–1606.
- (64) Hintermann, L.; Dang, T. T.; Labonne, A.; Kribber, T.; Xiao, L.; Naumov, P. *Chem.—Eur. J.* **2009**, *15*, 7167–7179.
- (65) Labonne, A.; Hintermann, K.; Hintermann, L. *Org. Lett.* **2006**, *25*, 5853–5856.
- (66) Grotjahn, D. B.; Lev, D. A. *J. Am. Chem. Soc.* **2004**, *126*, 12232–12233.
- (67) In most cases we have calculated TOF at high conversion (as opposed to using initial rates/conversions). The TOFs obtained in this manner are, presumably, underreported when compared to TOF based on initial rates as these are influenced by catalyst deactivation, product inhibition, and nitrile depletion (see Table 1-S). Catalyst **6** does exhibit a short induction period during the hydration of benzonitrile (see Supporting Information); the effect of the induction period is minimized in the calculation of TOF at high conversion.
- (68) (a) Daigle, D. J.; Pepperman, A. B., Jr.; Vail, S. L. *J. Heterocycl. Chem.* **1974**, *11*, 407–408. (b) Daigle, D. J. *Inorg. Synth.* **1998**, *32*, 40–45.
- (69) Taguchi, K.; Westheimer, F. H. *J. Org. Chem.* **1971**, *36*, 1570–1572.
- (70) Bennett, M. A.; Smith, A. K. *J. Chem. Soc., Dalton. Trans.* **1974**, 233–241.

NOTE ADDED IN PROOF

After acceptance of this manuscript, Tyler and co-workers published mechanistic details for ruthenium arene catalyzed nitrile hydration ([Organometallics dx.doi.org/10.1021/om301079u](https://doi.org/10.1021/om301079u)). Their work provides insight into the effect of $[\text{Cl}^-]$, ligand substitution, and Lewis basic ligands on nitrile hydration relevant to our work in this area.